Inelastic neutron scattering by coupled rotational and translational modes in CsCN

A Loidl†‡, K Knorr†‡, J I Kjems§ and S Haussühl‖

† Institut für Physik, Universität Mainz, 6500 Mainz, West Germany
§ Risø National Laboratory, 4000 Roskilde, Denmark
‖ Institut für Kristallographie, Universität zu Köln, 5000 Köln, West Germany

Caesium cyanide is a molecular crystal with a pseudocubic (CsCl) high-temperature phase ($a = 4.26$ Å). At 193 K CsCN transforms discontinuously into a trigonal (D_{3d}^5) structure (Dultz 1976, Sugisaki et al 1968). The CN^- molecules, which are orientationally disordered in the high-temperature phase, are now aligned along the threefold axis. In contrast to KCN and NaCN (which exhibit the rocksalt structure at high temperatures) no further phase transformation appears down to 14 K. This implies that the CN groups exist in a frozen-in state at low temperatures (Sugisaki et al 1968) with a residual disorder with respect to head and tail.

CsCN is not easy to produce in pure form owing to its strong hygroscopic behaviour, and work on this material has been very scarce. Apart from early x-ray data (Natta and Passerini 1931, Lely 1942) no spectroscopic data are available so far. In this Letter we will report inelastic neutron scattering data on the dynamics of transverse acoustic phonons which are coupled to low lying rotational excitations of the CN dumb-bells.

The single crystal of CsCN was grown from the melt employing the Czochralski technique and had a size of 0.3 cm³ with a mosaic spread of 0.4°. The measurements were carried out on a triple-axis spectrometer situated at the cold neutron source of the reactor DR3 at Risø. Fixed incident wavevectors k_i of 1.55 Å⁻¹ and of 2.66 Å⁻¹ were used with a pyrolytic graphite monochromator and analyser. Higher-order contaminations were reduced using common filter techniques. Typical horizontal collimations are 60′–40′–40′–40′ along the path of the neutrons. All scans were performed in the constant Q mode of operation within the (001) plane.

Figure 1 shows some representative scans along [110] T. The translational modes are well defined at small phonon wavevectors, broaden with increasing q and finally
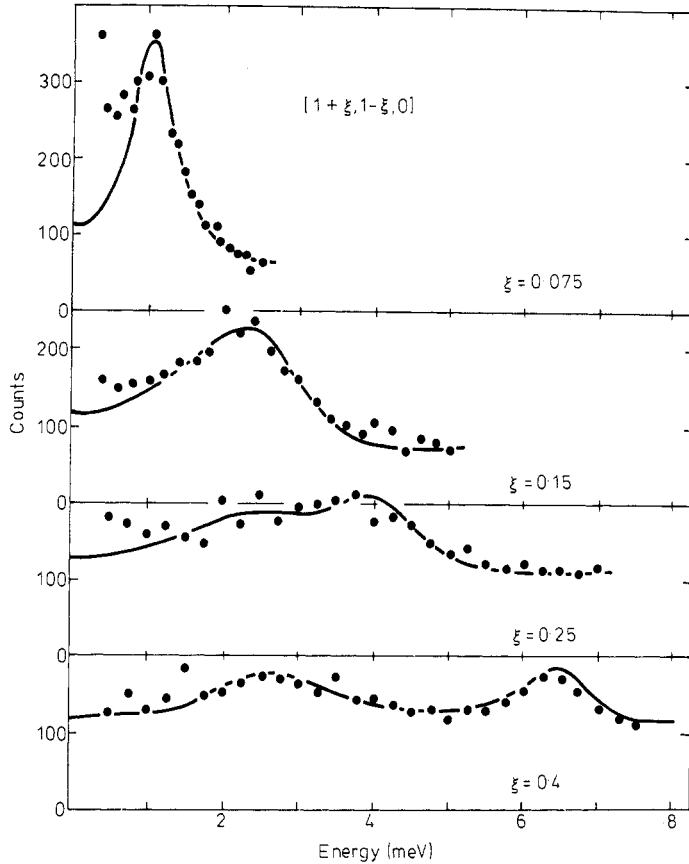
Figure 1. Neutron groups along [100] T collected with an incident wavevector $k_i = 1·55 \, \text{Å}^{-1}$ at room temperature (295 K). The lines are fits of the model to the experimental data.

anticross the rotational excitation. Near the zone boundary an acoustic phonon and a broad molecular excitation, centred at 3 meV, is observed. This result is another clear indication for the existence of a low lying internal mode in the high-temperature phase of the alkali cyanides. An analogous observation has been reported recently in KCN (Loidl *et al* 1980a, b). These scattered neutron groups can probably be related to the low-energy Raman bands in the low-temperature phases, that have been observed in KCN at 5·5 meV and at 4·5 meV in RbCN (Kondo *et al* 1979).

The drastic softening of transverse phonons propagating along [100] with decreasing temperatures is shown in figure 2 for a wavevector $q/q_{ZB} = 0·1$. This result is very similar to that obtained in KCN along the same symmetry direction (Rowe *et al* 1978, Loidl *et al* 1980a, b). Again the observed linewidths increase with the phonon wavevector, but in contrast to the observation in the [110] direction no spectroscopic evidence of a low lying molecular excitation could be detected. All of our results in CsCN at 295 K and at 223 K are summarised in figure 3. The excitation spectrum along [110] T_2 (E_g symmetry) corresponds to a mixed-mode picture with an increased mode–mode repulsion at the lower temperature. In the [100] T direction (T_{2g} symmetry) the centres of the neutron groups follow a sinusoidal q dependence with a softening that extends over the entire branch.
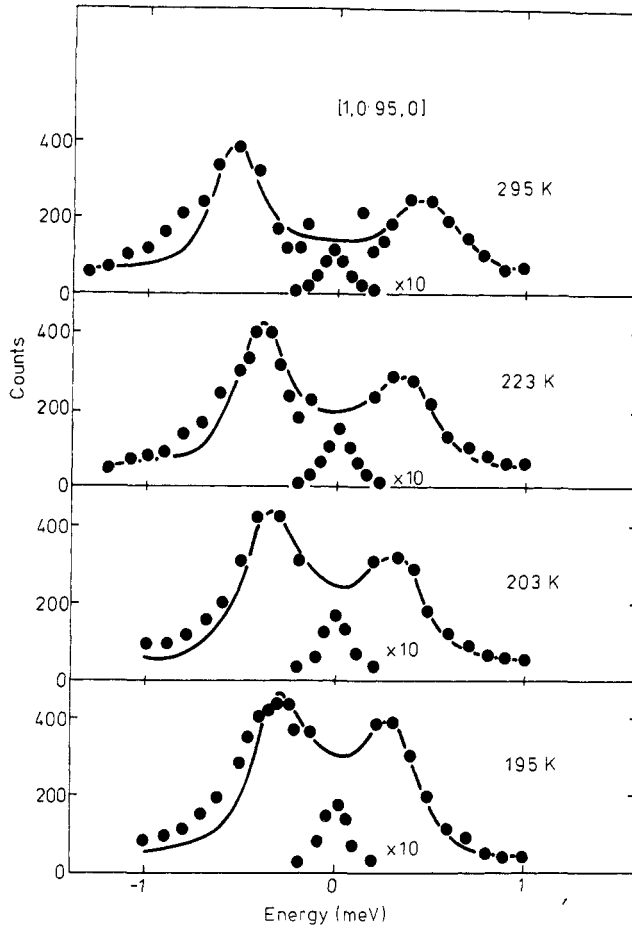
Figure 2. Neutron groups along [100] at four different temperatures (295 K, 223 K, 203 K, 195 K). Because of large Bragg tails we have chosen Q values which do not correspond to a purely transverse polarisation. The lines are the result of the theoretical model. The unexplained extra intensities at approximately 0·8 meV are due to the scattering of the longitudinal mode.

The results can be interpreted by a theory of Fulde (1978) on the magnetoelastic properties of rare earth systems with crystal field-split $4f^n$ states, which was subsequently applied to the dynamical properties of KCN (Loidl *et al* 1980a, b).

The starting point of the formalism is the single-ion susceptibility $g(\omega)$. In the case of one single transition of the energy transfer $\hbar\Delta$ and in the limit of high temperature $(T \gg \hbar\Delta/k_B)$, $g(\omega)$ is given by (Fulde 1978)

$$g(\omega) = -\frac{\hbar\tilde{O}^2}{2k_B T}\frac{\Delta^2}{\omega^2 - \Delta^2 + i\gamma\omega}. \tag{1}$$

In this magnetic analogue the eigenstates of the CN^- molecules which are determined from a single-ion Hamiltonian consisting of a free rotator term and the Devonshire potential of cubic symmetry (Beyeler 1972) correspond to the crystal field states of the 4f electrons. The transitions between the single-ion states have to be considered as a quadrupolar type, of T_{2g} and E_g symmetry with a strength determined by the transition
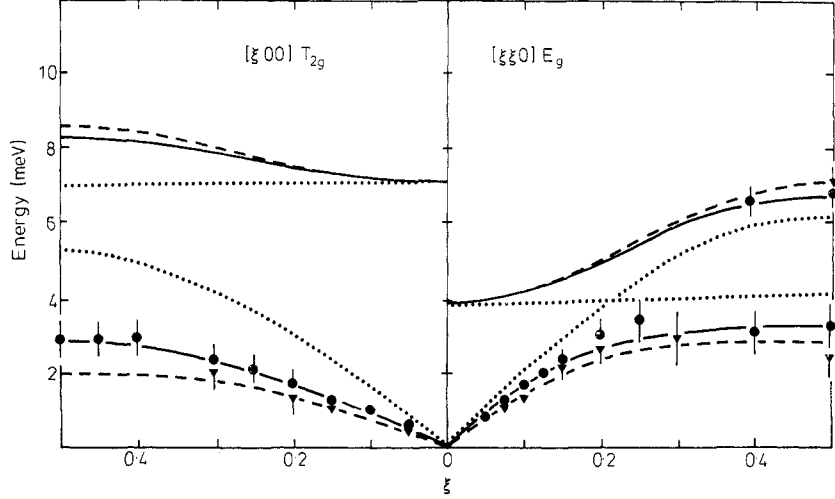
Figure 3. Dispersion relation in CsCN along [100] T and [110] T at 295 K (●) and at 223 K (▼) compared to the calculated values (dotted curve, undisturbed modes; full curve, coupled modes at 295 K; broken curve, coupled modes at 223 K).

matrix element $\tilde{O}^2$. In addition they are characterised by a linewidth γ due to damping effects. In principle one should introduce an effective coupling between neighbouring CN dumb-bells. This interaction would renormalise the single-ion susceptibility (Fulde 1978, Loidl et al 1980a, b). However, the analysis of our data shows that this additional parameter is not needed.

The phonon propagator of a particular symmetry in the presence of molecular excitations is given (Fulde 1978) by

$$D(\boldsymbol{q}, \omega) = \frac{2\omega_0(\boldsymbol{q})}{\omega_0^2(\boldsymbol{q}) - \omega^2 - 2A^2\omega_0^2(\boldsymbol{q})\, g(\omega)}. \tag{2}$$

where $\omega_0(\boldsymbol{q})$ is the undisturbed frequency and A^2 is the coupling constant between translational and rotational excitations. The poles of $D(\boldsymbol{q}, \omega)$ determine the excitations of the system which, in the limit of small damping, follow a simple mixed-mode picture. Using $\omega_0^2(\boldsymbol{q}) = (c_0/\rho)|\boldsymbol{q}|$ and $\omega^2 = (c/\rho)|\boldsymbol{q}|$ (with c_0 the undisturbed elastic constant, c the elastic constant in the presence of internal modes and ρ the mass density) the denominator of equation (2) yields, in the limits of $\omega \to 0$ and $q \to 0$, the well known result

$$c = c_0(T - T_{\mathrm{S}})/T. \tag{3}$$

At the characteristic temperature $T_{\mathrm{S}} = (\hbar/k_{\mathrm{B}})\, A^2\tilde{O}^2$ the elastic constant c vanishes. Finally the dynamic structure factor is determined by

$$S(\boldsymbol{q}, \omega) = [1 - \exp(-\beta\omega)]^{-1} \operatorname{Im} D(\boldsymbol{q}, \omega). \tag{4}$$

The full curves in figures 1 and 2 represent the best fit of equation (4) to the experimental data points, where we included the spectrometer efficiency for fixed incoming neutron energies. The dispersion of the bare phonon frequencies $\omega_0(\boldsymbol{q})$ was simply assumed to follow a sinusoidal dependence with the initial slope determined by the background elastic constant c_0. The agreement between theory and experiment is satisfactory and the parameters as determined from these fits are listed in table 1. The values of the parameters

Table 1. Parameters determined by a fit of the theoretical model to the observed neutron lineshapes in T_{2g} and E_g symmetries.

Symmetry	T_{2g}	E_g
c_0 ($\times 10^{10}$ dyn cm^{-2})	$8 \cdot 3 \pm 0 \cdot 7$	$5 \cdot 4 \pm 0 \cdot 3$
T_S (K)	$155 \cdot 0 \pm 6 \cdot 0$	$97 \cdot 0 \pm 5 \cdot 0$
Δ (meV)	$7 \cdot 0 \pm 1 \cdot 5$	$3 \cdot 8 \pm 0 \cdot 6$
γ (meV)	$4 \cdot 0 \pm 1 \cdot 0$	$2 \cdot 7 \pm 0 \cdot 5$

for the T_{2g} symmetry modes were derived from fits to data of figure 2 and to the neutron lineshapes at larger wavevectors. Obviously, the E_g and the T_{2g} translational modes couple to different rotational excitations, a behaviour that was also observed in the mixed molecular system $KBr_{1-x}(CN)_x$ (Loidl et al 1980a, b). It is interesting to note that no anomalous dispersion was found for the T_{2g} mode of CsCN in contrast to the results in KCN and NaCN (Rowe et al 1975). The applied formalism offers a straight-forward explanation. In the limit $\Delta \gg \omega$, equation (1) yields

$$g(\omega) = \frac{\hbar \tilde{O}^2}{2 k_B T} \frac{1}{(1 - \omega \tau)} \tag{5}$$

where the two originally independent parameters Δ and γ are replaced by the relaxational time $\tau = \gamma/\Delta^2$. This limit corresponds to the relaxational *ansatz* commonly used to explain the dynamics of molecular systems (Rowe et al 1978, Yamada et al 1974). With this relaxational-type single-ion susceptibility, the poles of the translational modes are at

$$\omega^2 = \omega_0^2 (T - T_S)/T \qquad \text{for } \omega \tau \ll 1 \tag{6}$$

and at

$$\omega^2 = \omega_0^2 \qquad \text{for } \omega \tau \gg 1. \tag{7}$$

The parameters of table 1 and figure 3 show that all the phonon frequencies of the [100] TA branch in CsCN roughly fall into the range of fast relaxation (Yamada et al 1974) $\omega \tau \ll 1$. This explains immediately the softening of the sound velocities according to equation (6). Of course, the relaxational *ansatz* strictly holds for the small phonon frequencies near the zone centre only. Near the zone boundary $\omega \tau$ is about $0 \cdot 4$ and ω is of the order of Δ; here a better overall fit could be obtained by utilising the two parameters Δ and γ of table 1 instead of the relaxation time τ, although it has to be mentioned that the parameters c_0, Δ and γ were strongly correlated as can be seen from the estimated errors.

Figure 3 shows the dispersion relation for the coupled modes which were calculated from the denominator of equation (2), using the parameters c_0, Δ and T_S of table 1, but neglecting lifetime effects (i.e. $\gamma = 0$). Larger deviations from apparent peak positions of the experiment occur only in E_g symmetry near the resonance frequency of the mixed modes, where large lifetimes of the modes simulate an S-shaped dispersion rather than a double peak structure of well defined excitations. Finally, figure 4 shows the prediction of the present model for the temperature dependence of the elastic constants c_{44} and $(c_{11} - c_{12})/2$, calculated according to equation (4) with the parameters T_S and c_0 of table 1. Of course, these calculated elastic constants coincide quite well with the values as determined from the slopes of the long-wavelength phonons (see for instance figure 2).

In conclusion, we have presented inelastic neutron scattering data which show clearly the effects of a coupling of translational modes to internal degrees of freedom of the CN^- molecules. All the data could be explained by approximating the molecular susceptibility by a single Van Vleck term including line broadening. Along [110] T the relevant rotational transition is within the frequency range of the acoustic mode and causes a mixed-mode behaviour; in the [100] T direction the observed translational excitations give
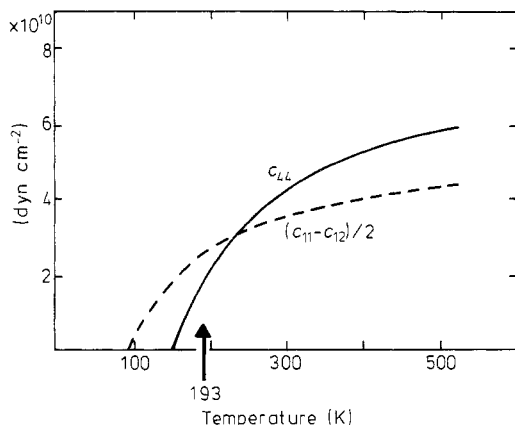

Figure 4. Temperature dependence of the elastic constants c_{44} and $(c_{11} - c_{12})/2$ predicted by the model of this work. The arrow at 193 K indicates the actual transition temperature (Sugisaki *et al* 1968).

clear evidence of being coupled to a nearly relaxational type susceptibility in the limits of fast relaxation $\omega\tau \ll 1$. The phase transition in CsCN at 193 K occurs, similar to that in KCN (Rowe *et al* 1978, Loidl *et al* 1980a, b), because of the coupling between translational modes and internal molecular states of T_{2g} symmetry. Hence it belongs to the class of transitions which can be described theoretically by the coupling of a pseudospin variable, in this case the CN^- orientation, and the phonons of the host lattice. Other examples belonging to this class are the transitions in the hydrogen-bonded ferroelectrics (Kobayashi 1968) and the cooperative Jahn–Teller transitions which take place in a number of rare earth salts (Gehring and Gehring 1975).

References

Beyeler H U 1972 *Phys. Stat. Solidi* (b) **52** 419
Dultz W 1976 *Habilitationsschrift* Regensburg
Fulde P 1978 *Handbook on the Physics and Chemistry of Rare Earths* ed K A Gschneidner Jr and L Eyring (Amsterdam: North-Holland) p 295
Gehring G A and Gehring K A 1975 *Rep. Prog. Phys.* **38** 1
Kobayashi K K 1968 *J. Phys. Soc. Japan* **24** 297
Kondo Y, Schoemaker D and Lüthy F 1979 *Phys. Rev.* B **19** 4210
Lely J A 1942 *Dissertation* Utrecht
Loidl A, Feile R, Knorr K, Renker R, Daubert J, Durand D and Suck J B 1980a *Z. Phys.* to be published

Loidl A, Knorr K, Daubert J, Dultz W and Fitzgerald W J 1980b *Z. Phys.* B in press
Natta G and Passerini L 1931 *Gazz. Chim. Ital.* **61** 191
Rowe J M, Rush J J, Chesser N J, Michel K H and Naudts J 1978 *Phys. Rev. Lett.* **40** 455
Rowe J M, Rush J J, Vegelatos N, Prince D L, Hinks D G and Susman S 1975 *J. Chem. Phys.* **62** 4551
Sugisaki M, Matsuo T, Suga H and Seki S 1968 *Bull. Chem. Soc. Japan* **41** 1747
Yamada Y, Taktera H and Huber D L 1974 *J. Phys. Soc. Japan* **36** 641